

Aspects of Dirac Physics in Graphene

K. Sengupta

*Indian Association for the Cultivation of
Sciences, Kolkata*

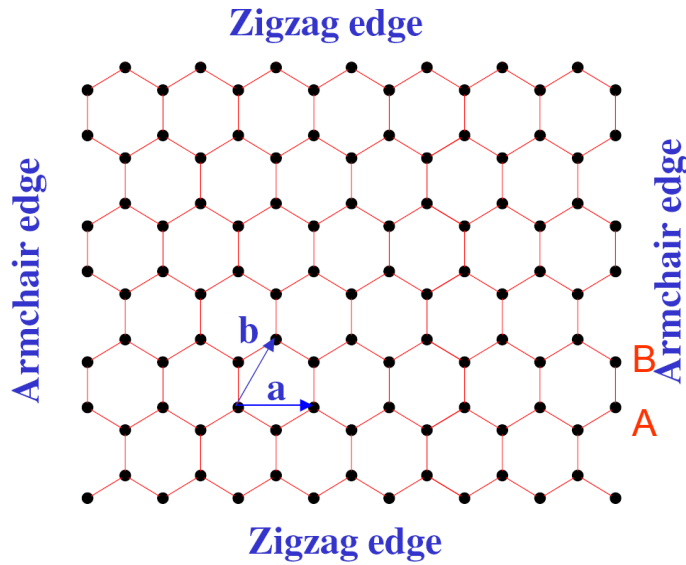


Overview

1. Origin of Dirac physics in graphene
2. Superconducting junctions
3. Physics of graphene junctions
4. Kondo physics and STM spectroscopy in graphene
5. Conclusion

Origin of Dirac physics in graphene

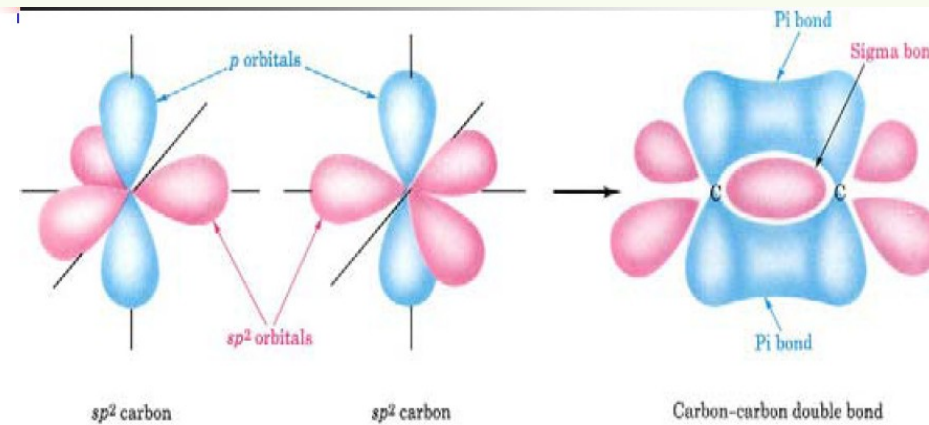
Relevant Basics about graphene



Honeycomb lattice

Tight binding model for graphene with nearest neighbor hopping.

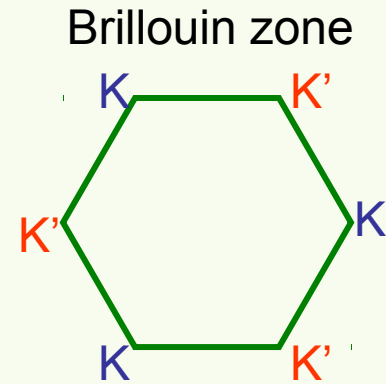
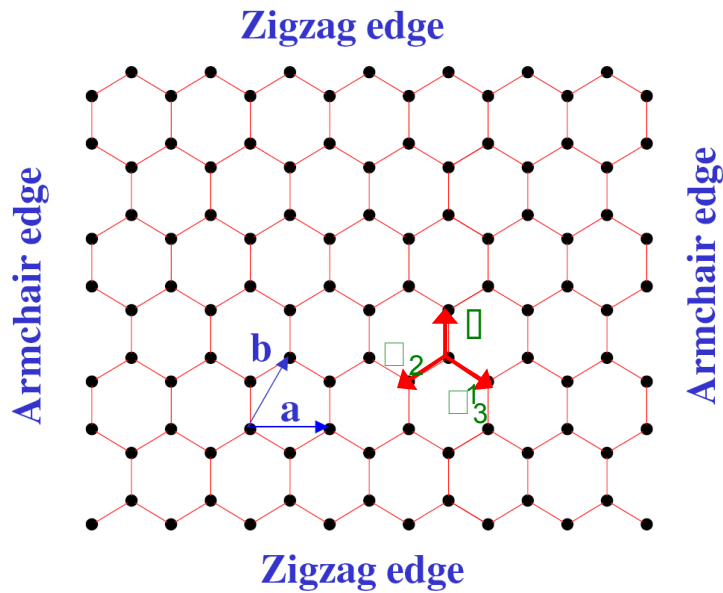
Can in principle include next-nearest neighbor hopping: same low energy physics. Ref: [arXiv:0709.1163](https://arxiv.org/abs/0709.1163)



Each unit cell has two electrons from $2p_z$ orbital leading to **delocalized π bond**.

$$H = \int d^2x \psi^\dagger \begin{pmatrix} 0 & \hat{t} \\ \hat{t}^* & 0 \end{pmatrix} \psi$$

$$\psi = (\psi_A, \psi_B)$$



Diagonalize in momentum space
to get the energy dispersion.

$$H = \int d^2k \psi^\dagger(\mathbf{k}) \begin{pmatrix} 0 & h(\mathbf{k}) \\ h^*(\mathbf{k}) & 0 \end{pmatrix} \psi(\mathbf{k})$$

$$h(\mathbf{k}) = -t \sum_{j=1}^3 e^{-i\mathbf{k} \cdot \boldsymbol{\tau}_j}$$

Energy dispersion: $E_{\pm}(\mathbf{k}) = \pm E(\mathbf{k}) = \pm |h(\mathbf{k})|$

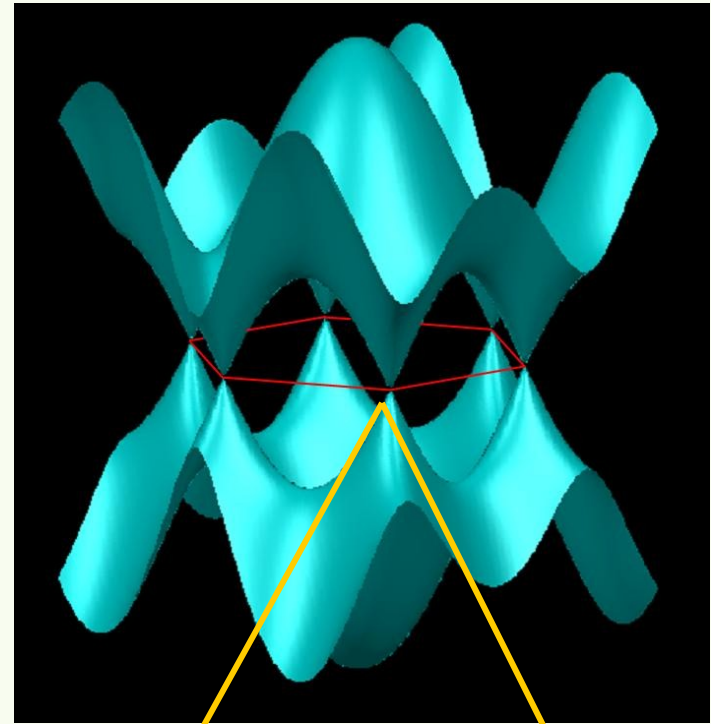
There are two energy bands
(valence and conduction)
corresponding to energies $\pm E(\mathbf{k})$

These two bands touch each other
at six points at the edges of the
Brillouin zone

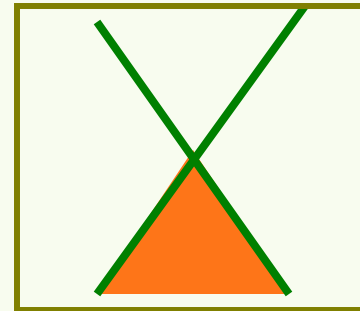
Two of these points K and K'
are inequivalent; rest are related by
translation of a lattice vector.

Two inequivalent Fermi points
rather than a Fermi-line.

Dirac cone about the K and K' points



$$E(\mathbf{k}) \simeq \pm v_F |\mathbf{k}|$$



Thus at low energies one can think of a four component wave function for the low-energy quasiparticles (sans spin).

$$\psi = (\psi_A^K, \psi_B^K, \psi_A^{K'}, \psi_B^{K'})$$

<i>Terminology</i>	<i>Pauli matrix</i>	<i>Relevant space</i>
Pseudospin	σ	2 by 2 matrix associated with two sublattice structure
Valley	τ	2 by 2 matrix associated with two BZ points K and K'
Spin	S	2 by 2 matrix associated with the physical spin.

$$\mathcal{H}_a = \int d^2k \psi^\dagger v_F (\tau_3 \sigma_x k_x + \sigma_y k_y) \psi$$



At each valley, we have a massless Dirac eqn. with Dirac matrices replaced by Pauli matrices and c replaced by v_F .

No large k scattering leads to two species of massless Dirac Fermions.

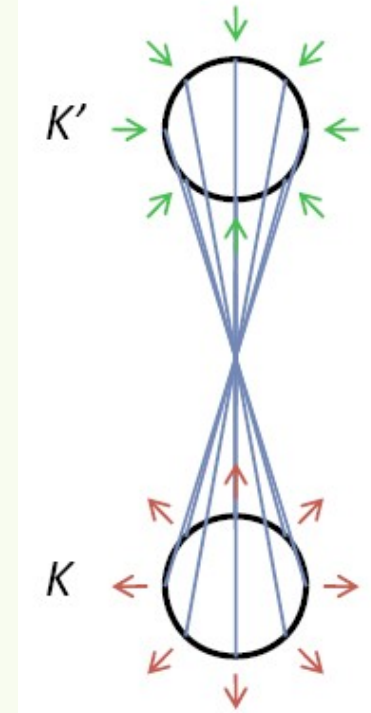
Helicity associated with Dirac electrons at K and K' points.

Solution of H_a about K point:

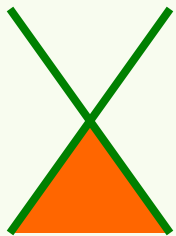
$$\psi_K \simeq (1, \pm e^{i\gamma})$$

$$\gamma = \tan^{-1}(k_y/k_x)$$

Electrons with $E > 0$ around K point have their pseudospin along \mathbf{k} where pseudospin refers to A-B space. For K', pseudospin points opposite to \mathbf{k} .

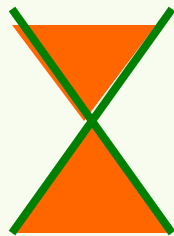


$E_F = 0$



Zero doping
Fermi point

$E_F > 0$



Finite doping
Fermi surface

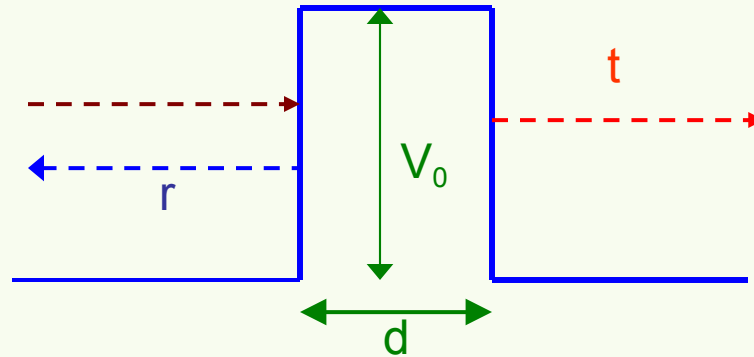


E_F can be tuned by an external gate voltage.

DOS varies linearly with E for undoped graphene but is almost a constant at large doping. $\rho(E) \sim |E - E_F|$

Within RG, interactions are (marginally) irrelevant.

Dirac nature II: Potential barriers in graphene



Simple Problem: What is the probability of the incident electron to penetrate the barrier?

Solve the Schrodinger equation and match the boundary conditions

Answer:

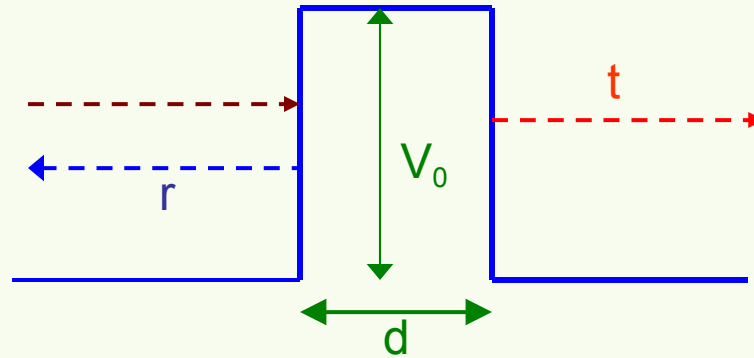
$$T = |t|^2 = \frac{4\chi^2 k^2}{4\chi^2 k^2 + (k^2 + \chi^2)^2 \sinh^2(\chi)}$$

where

$$\chi = \frac{2(V_0 - E)d}{\hbar v_d}, \quad v_d = \hbar/md, \quad k^2 = 2md^2 E/\hbar^2$$

Basic point: For $V_0 \gg E$, T a monotonically decreasing function of the dimensionless barrier strength.

Simple QM 102: A 2D massless Dirac electron in a potential barrier



$$T_D = |t|^2 = \frac{\cos^2(\gamma)}{1 - \cos^2(\chi) \sin^2(\gamma)}$$

$$\chi = \frac{V_0 d}{\hbar v_F},$$

$$\tan(\gamma) = k_y / k_x$$

For normal incidence, $T=1$.
Klein paradox for Dirac electrons.
 Consequence of inability of a scalar potential to flip pseudospin

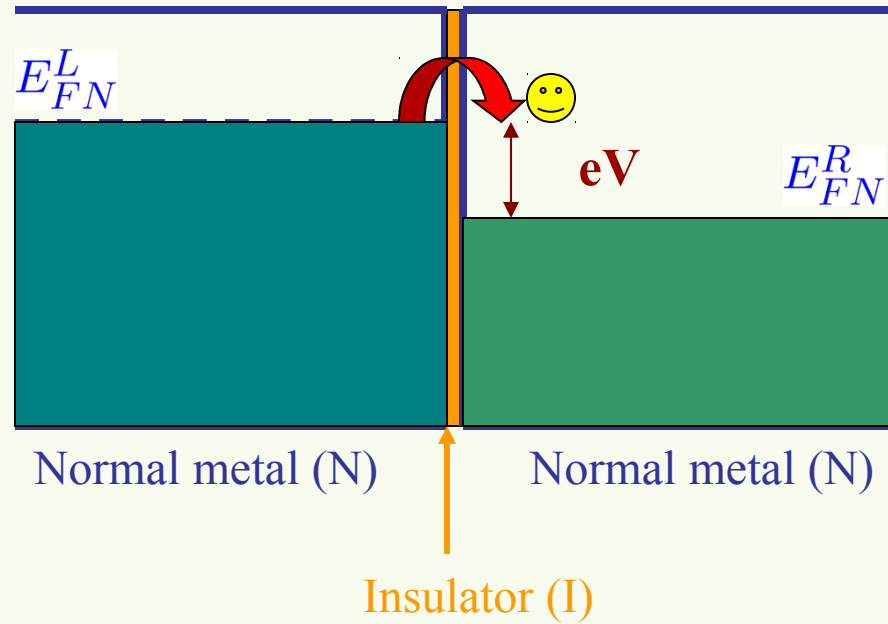
For any angle of incidence $T=1$ if
 $\chi = n\pi$ **Transmission resonance**
 condition for Dirac electrons.

Basic point: T is an oscillatory function of the dimensionless barrier strength.
 Qualitatively different physics from that of the Schrödinger electrons.

Conventional Superconducting junctions

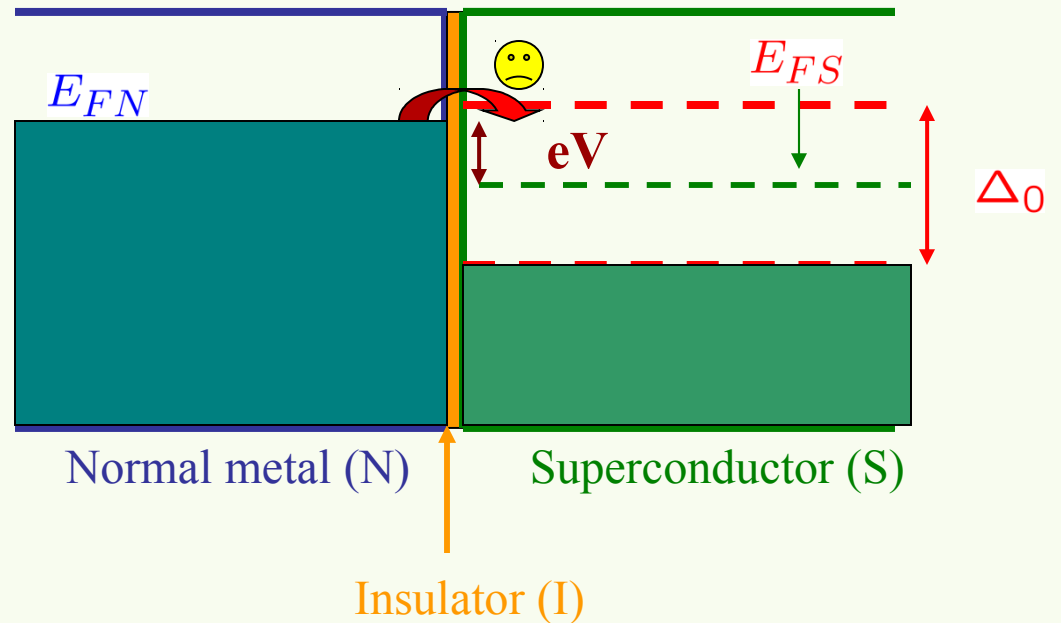
Superconductivity and tunnel junctions

N-I-N interface



Measurement of tunneling conductance

N-I-S interface

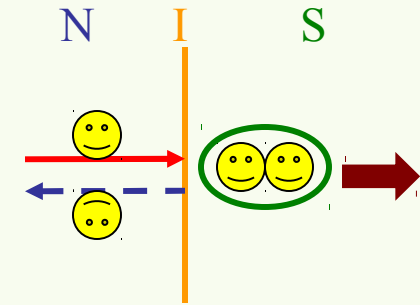


Basic mechanism of current flow in a N-I-S junction

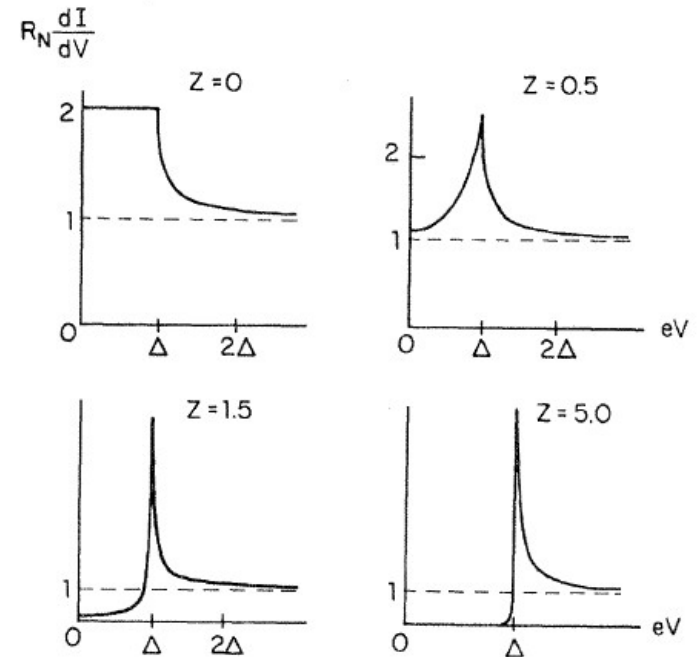
Andreev reflection is strongly suppressed in conventional junctions if the insulating layer provides a large potential barrier: so called tunneling limit

In conventional junctions, subgap tunneling conductance is a monotonically decreasing function of the effective barrier strength Z .

Zero bias tunneling conductance decays as $1/(1+2z^2)^2$ with increasing barrier strength.



Andreev reflection
2e charge transfer



Josephson Effect

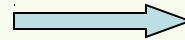


The ground state wavefunctions have different phases for S_1 and S_2



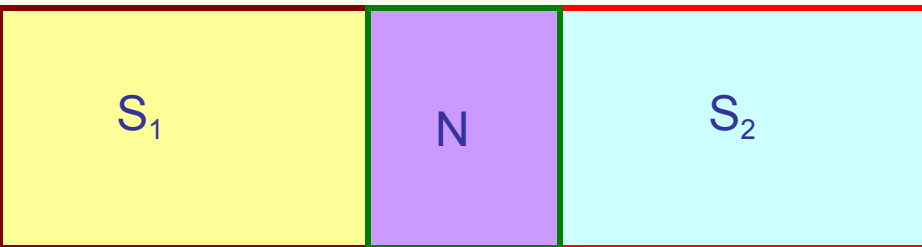
$$\begin{aligned}\psi_1 &\sim e^{i\phi_1} \\ \psi_2 &\sim e^{i\phi_2}\end{aligned}$$

Thus one might expect a current between them: **DC Josephson Effect**

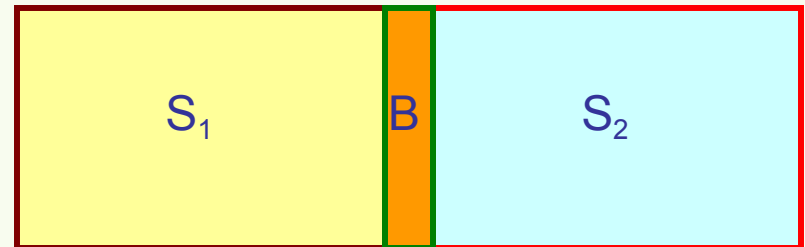


$$j \sim \text{Im}[\psi_1^* \psi_2] \sim \sin(\phi_2 - \phi_1)$$

Experiments: Josephson junctions [Likharev, RMP 1979]

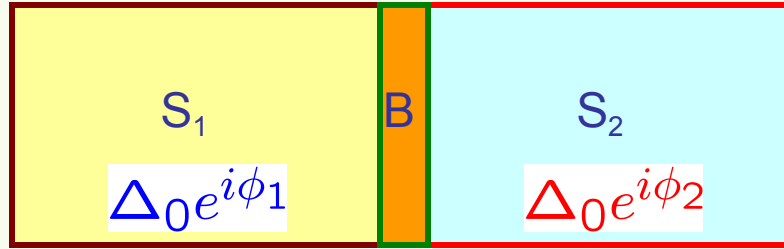


S-N-S junctions or weak links



S-B-S or tunnel junctions

Josephson effect in conventional tunnel junctions



Formation of localized subgap Andreev bound states at the barrier with energy dispersion which depends on the phase difference of the superconductors.

$$E_{\pm} = \pm \Delta_0 \sqrt{1 - T \sin^2(\phi/2)},$$

$$T = 4/(4 + Z^2),$$

Z is the dimensionless barrier strength.

The primary contribution to Josephson current comes from these bound states.

$$I = \frac{2e}{\hbar} \sum_{n=\pm} \sum_{k_{\parallel}} \frac{\partial E_n}{\partial \phi} f(E_n/k_B T_0)$$

Kulik-Omelyanchuk limit:

$$T \rightarrow 1 \quad I(T_0 = 0) \sim |\sin(\phi/2)|$$

$$I_c R_N = \pi \Delta_0 / e$$

Ambegaokar-Baratoff limit:

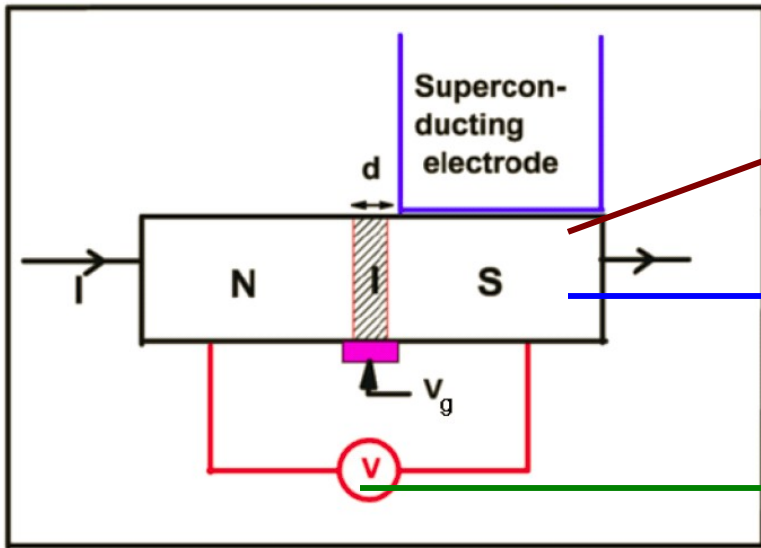
$$T \rightarrow 0 \quad I(T_0 = 0) \sim T \sin(\phi)$$

$$I_c R_N = \pi \Delta_0 / 2e$$

Both I_c and $I_c R_N$ monotonically decrease as we go from KO to AB limit.

Graphene Junctions

Graphene N-B-S junctions



Superconductivity is induced via proximity effect by the electrode.

Effective potential barrier created by a gate voltage V_g over a length d . Dimensionless barrier strength: $\chi = V_g d / (\hbar v_F)$

Applied bias voltage V .

Dirac-Bogoliubov-de Gennes (DBdG) Equation

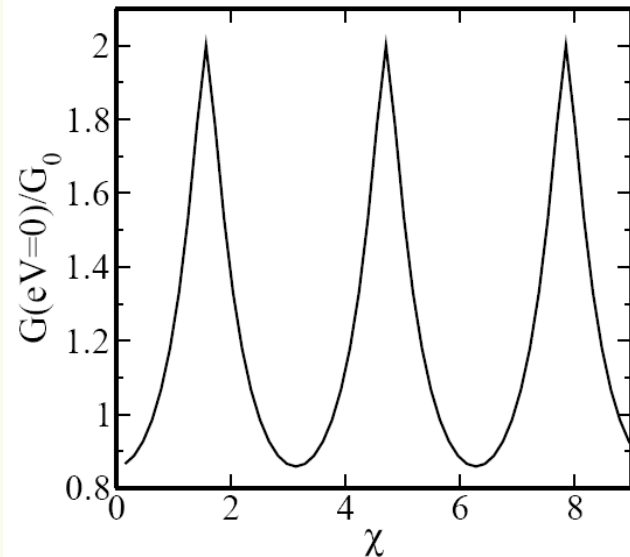
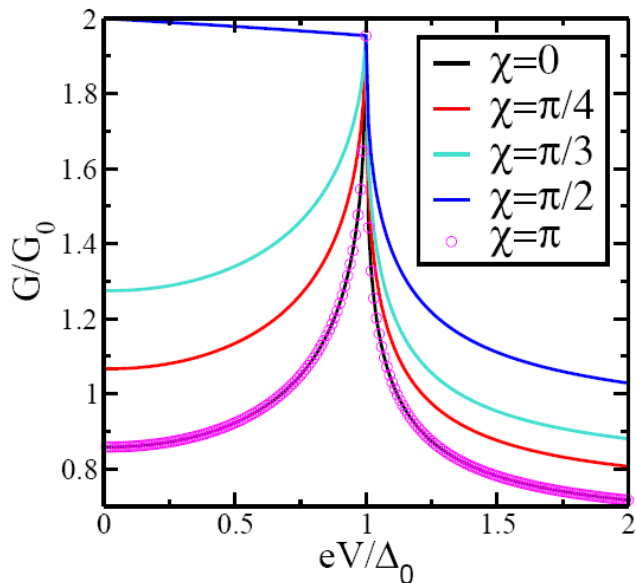
$$\begin{pmatrix} \mathcal{H}_a - E_F + U(\mathbf{r}) & \Delta(\mathbf{r}) \\ \Delta^*(\mathbf{r}) & E_F - U(\mathbf{r}) - \mathcal{H}_a \end{pmatrix} \psi_a = E \psi_a.$$

- $E_F \longrightarrow$ Fermi energy
- $U(\mathbf{r}) \longrightarrow$ Applied Potential = V_g for $0 > x > -d$
- $\Delta(\mathbf{r}) \longrightarrow$ Superconducting pair-potential between electrons and holes at K and K' points

Question: How would the tunneling conductance of such a junction behave as a function of the gate voltage?

Results in the thin barrier limit

Central Result: In complete contrast to conventional NBS junction, Graphene NBS junctions, due to the presence of Dirac-like dispersion of its electrons, exhibit novel π periodic oscillatory behavior of subgap tunneling conductance as the barrier strength is varied.



π periodic oscillations of subgap tunneling conductance as a function of barrier strength $\tilde{\chi}$

Tunneling conductance maxima occur at $\tilde{\chi} = (n+1/2)\pi$

Transmission resonance condition

Maxima of conductance occur when $r=0$.

$$G = G_0 \int_0^{k_F} \frac{dk_{\parallel}}{2\pi} (1 - |r|^2 + |r_A|^2)$$

For subgap voltages, in the thin barrier limit, and for $eV \ll E_F$, it turns out that

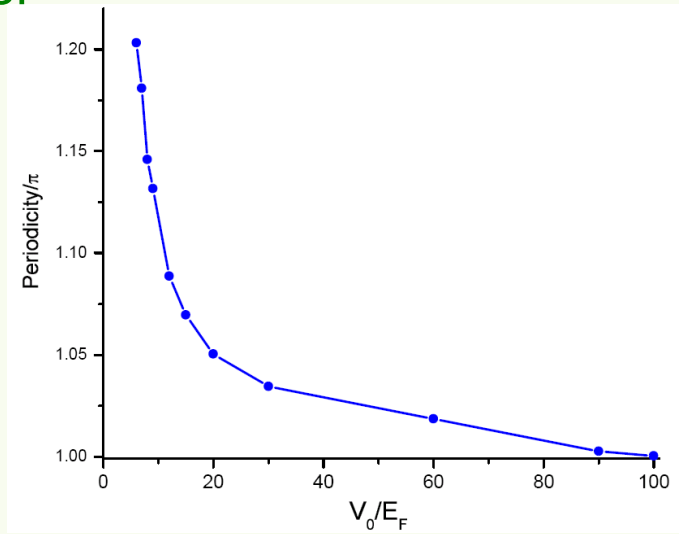
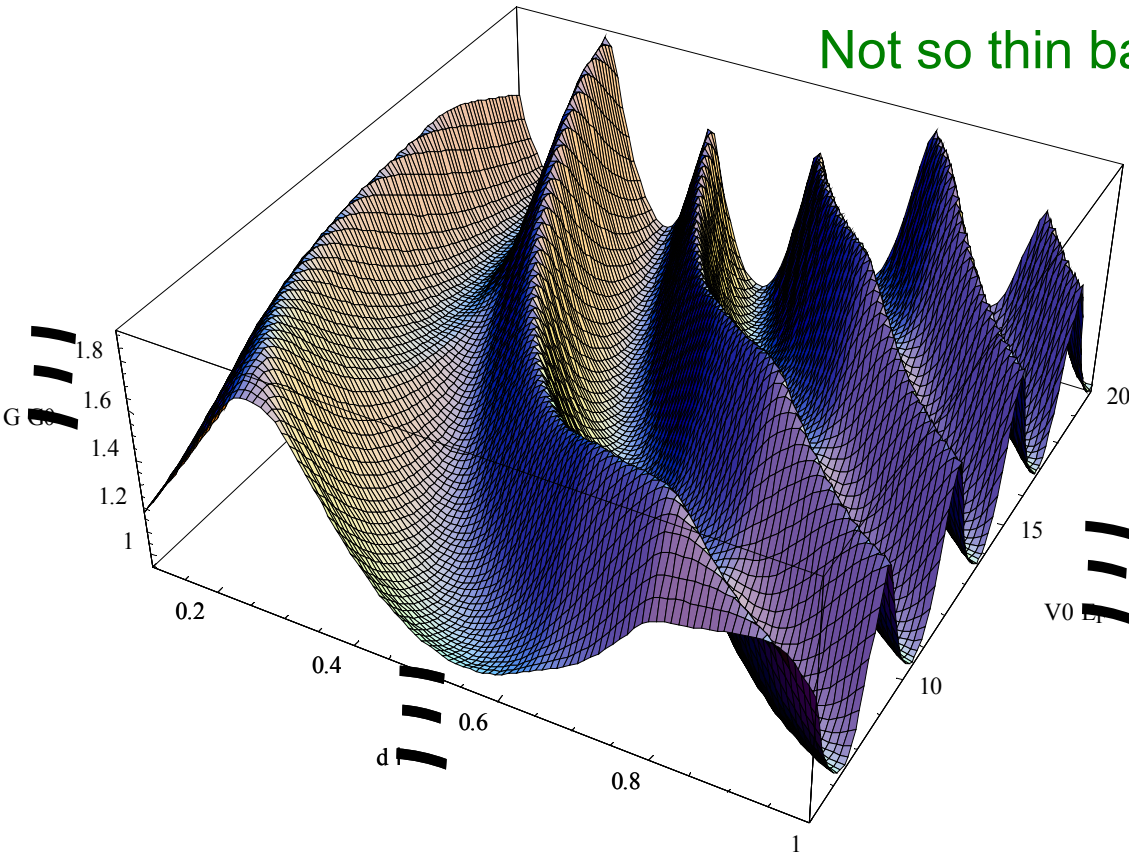
$$r \sim \sin(\gamma) \cos(\chi) \sin(\beta)$$

where $\cos(\beta) = eV/\Delta_0$ and $\gamma = \sin^{-1}[\hbar v_F k_{\parallel}/(eV + E_F)]$ is the angle of incidence

$r=0$ and hence G is maximum if:

1. $\chi = 0$: Manifestation of Klein Paradox. Not seen in tunneling conductance due to averaging over transverse momenta.
2. $\beta = 0$: Maxima of tunneling conductance at the gap edge: also seen in conventional NBS junctions.
3. $\beta = (n+1/2)\pi$: Novel transmission resonance condition for graphene NBS junction.

Not so thin barrier



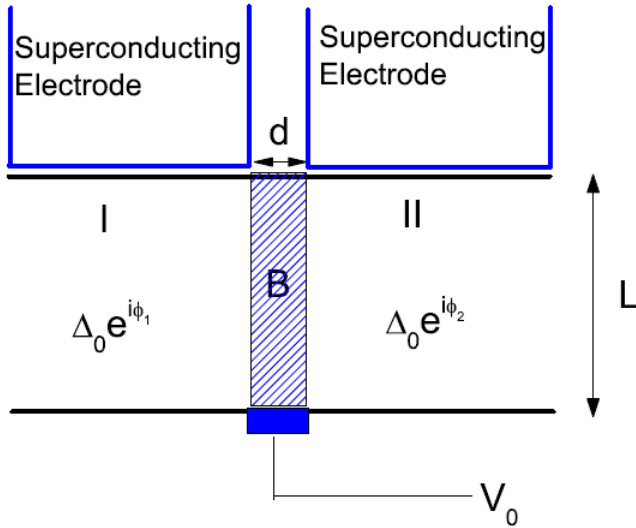
Oscillations persists: so one expects the oscillatory behavior both as functions of V_G and d to be robust.

However, the maximum value of G may be lesser than the Andreev limit value of $2G_0$

The periodicity of the oscillations shall vary with V_G and will deviate from $\tilde{\square}$

Graphene S-B-S junctions

Schematic Setup



$$\begin{pmatrix} \mathcal{H}_a - E_F + U(\mathbf{r}) & \Delta(\mathbf{r}) \\ \Delta^*(\mathbf{r}) & E_F - U(\mathbf{r}) - \mathcal{H}_a \end{pmatrix} \psi_a = E \psi_a.$$

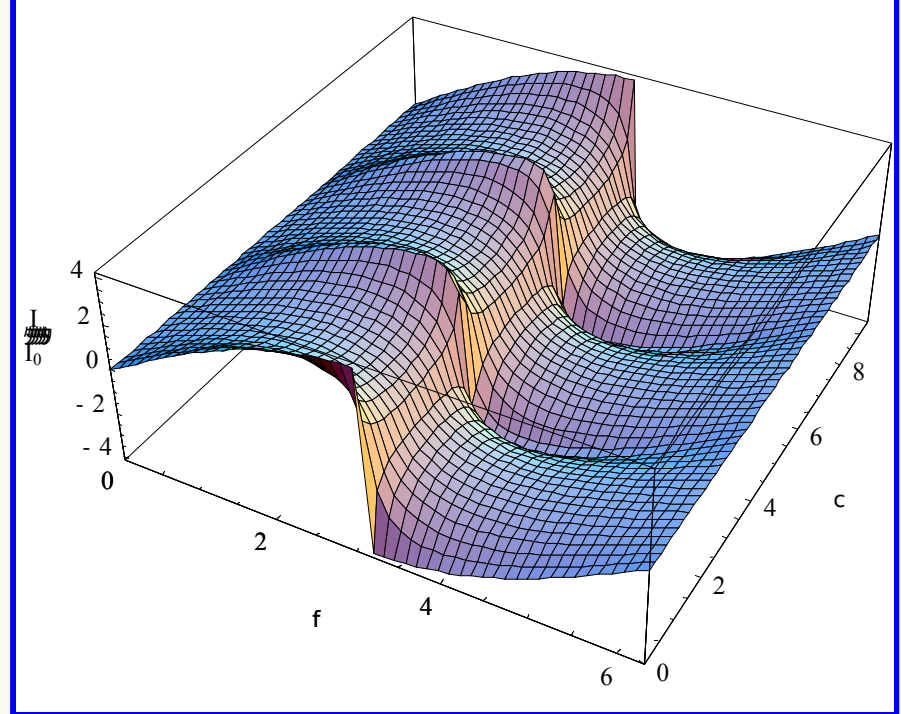
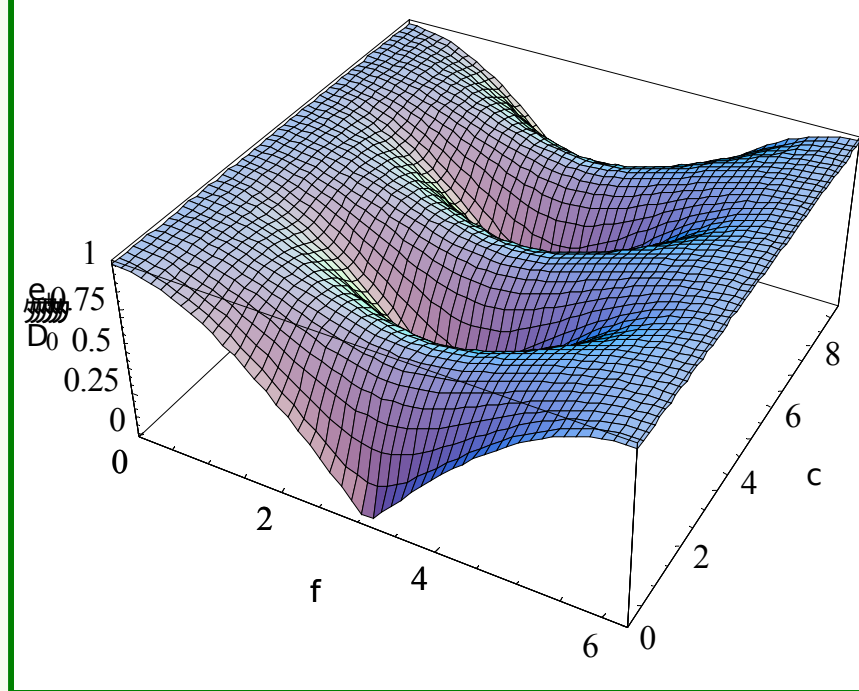
E_F Fermi energy
 $U(\mathbf{r})$ Applied Potential = V_0 for $0 > x > -d$
 $\Delta(\mathbf{r})$ Superconducting pair-potential in regions I and II as shown

Question: How would the Josephson current behave as a function of the gate voltage V_0



Procedure:

1. Solve the DBdG equation in regions I, II and B.
2. Match the boundary conditions at the boundaries between regions I and B and B and II.
3. Obtain dispersion for bound Andreev subgap states and hence find the Josephson current.



$$\epsilon_{\pm}(q, \phi; \chi) = \pm \Delta_0 \sqrt{1 - T(\gamma, \chi) \sin^2(\phi/2)},$$

$$T(\gamma, \chi) = \frac{\cos^2(\gamma)}{1 - \cos^2(\chi) \sin^2(\gamma)}.$$

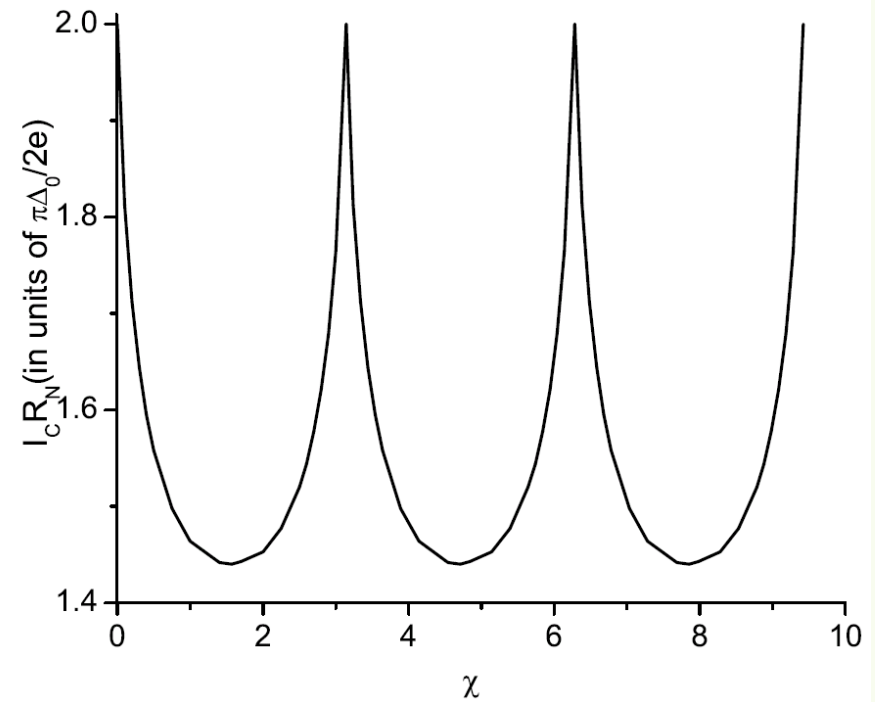
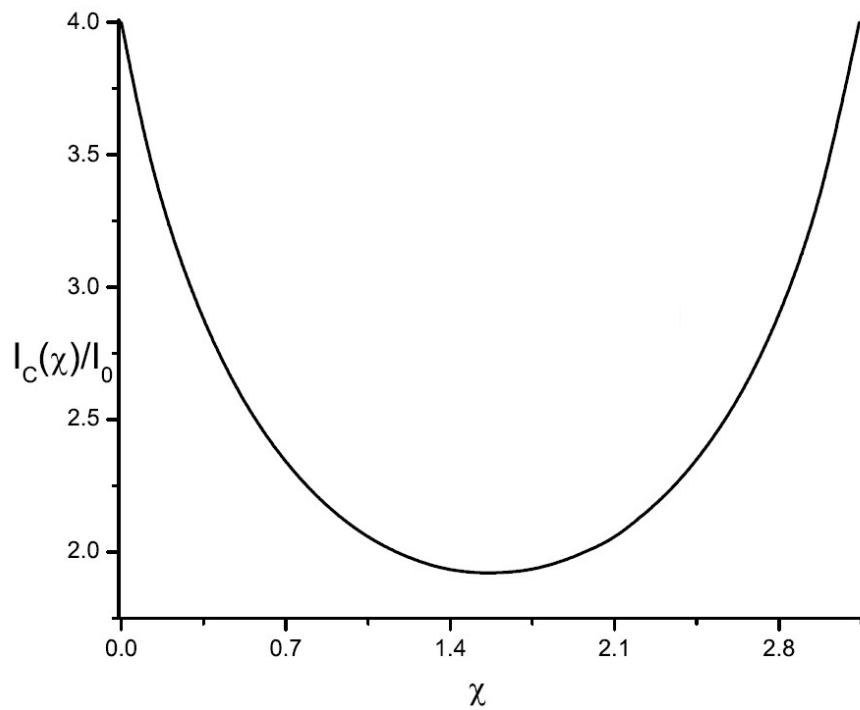
$$\sin(\gamma) = \hbar v_F q / E_F$$

$$I(\phi, \chi, T_0) = I_0 g(\phi, \chi, T_0)$$

$$g(\phi, \chi, T_0) = \int_{-\pi/2}^{\pi/2} d\gamma \left[\frac{T(\gamma, \chi) \cos(\gamma) \sin(\phi)}{\sqrt{1 - T(\gamma, \chi) \sin^2(\phi/2)}} \times \tanh(\epsilon_+/2k_B T_0) \right].$$

DBdG quasiparticles has a transmission probability T which is an oscillatory function of the barrier strength $\tilde{\Delta}$

The Josephson current is an oscillatory function of the barrier strength $\tilde{\Delta}$



I_C and $I_C R_N$ are π periodic bounded oscillatory functions of the effective barrier strength

$I_C R_N$ is bounded with values between $\pi\Delta_0/e$ for $\chi = n\pi$ and $2.27\pi\Delta_0/e$ for $\chi = (n+1/2)\pi$.

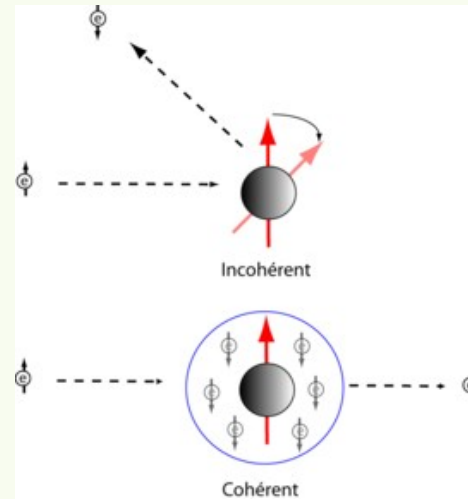
For $\chi = n\pi$, $I_C R_N$ reaches $\pi\Delta_0/e$:
Kulik-Omelyanchuk limit.

Due to transmission resonance of DBdG quasiparticles, it is not possible to make T arbitrarily small by increasing gate voltage V_0 . Thus, these junctions never reach Ambegaokar-Baratoff limit.

Kondo Physics and STM spectroscopy

Kondo effect in conventional systems

Metal + Magnetic Impurity



Formation of a many-body correlated state below a crossover temperature T_K , where the impurity spin is screened by the conduction electrons.

Features of Kondo effect:

1. Appropriately described by the Kondo model:
2. The coupling J , in the RG sense, grows at low T and becomes weak at high T .
Negative beta function.
Anderson *J. Phys. C* **3**, 2436–2441 (1970) .

$$H = H_0 + JS \cdot s(0)$$

$$\beta(J) = -\rho(E_F)J^2$$

$$T_K = D \exp(-1/\rho(E_F)J)$$

3. **For two or more channels of conduction electrons (multichannel) the resultant ground state is a non-Fermi liquid.**
For a single channel, the ground state is still a Fermi liquid.

4. **All the results depend crucially on the existence of constant DOS at E_F**
5. **Kondo state leads to a peak in the conductance at zero bias, as measured by STM.**

What's different for possible Kondo effect in graphene

For undoped graphene, linearly varying DOS makes a Kondo screened phase impossible [Casselano and Fradkin, Andersson, Polkovnikov, Sachdev and Vojta].

At finite and large doping, an effectively constant DOS occurs and hence one should see a Kondo screened phase.

One can tune into a Kondo screened phase by applying a gate voltage

$$k_B T^* = \Lambda \exp[(1 - J_c(0)/J)/(2q \ln[1/q^2])].$$
$$q = eV/\Lambda.$$

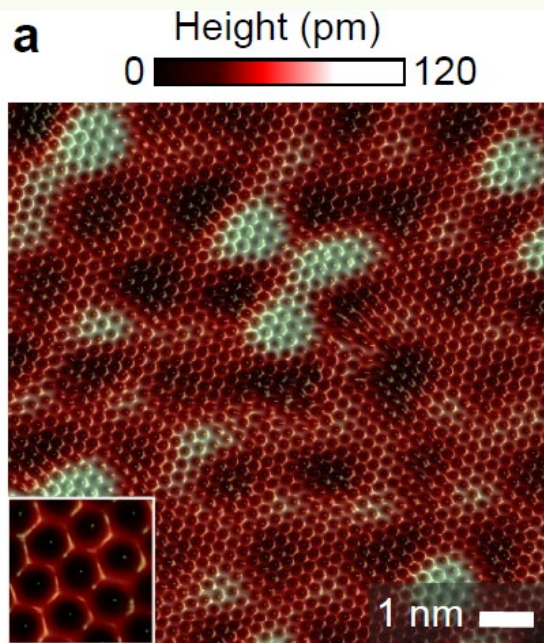
$J \simeq 2 \text{ eV}$ and voltage $eV \simeq 0.5 \text{ eV}$, $T^* \simeq 35 \text{ K}$.

Also, two species of electrons from K and K' points may act as two channels if the impurity radius is large enough so that large-momenta scatterings are suppressed.

Possibility of two-channel Kondo effect in graphene.

Theoretical prediction: Sengupta and Baskaran PRB (2007)

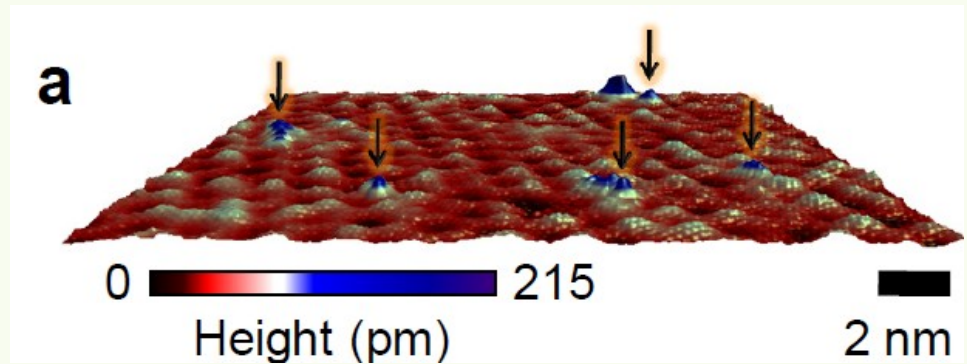
Recent STM experiments on doped graphene



**Constant current STM topography
of pure graphene (100 nm^2 $I=40\text{pA}$)**



**Typical parameters:
 $E_F=250\text{meV}$ and $T=4\text{K}$.**



Adding Cobalt impurity in graphene

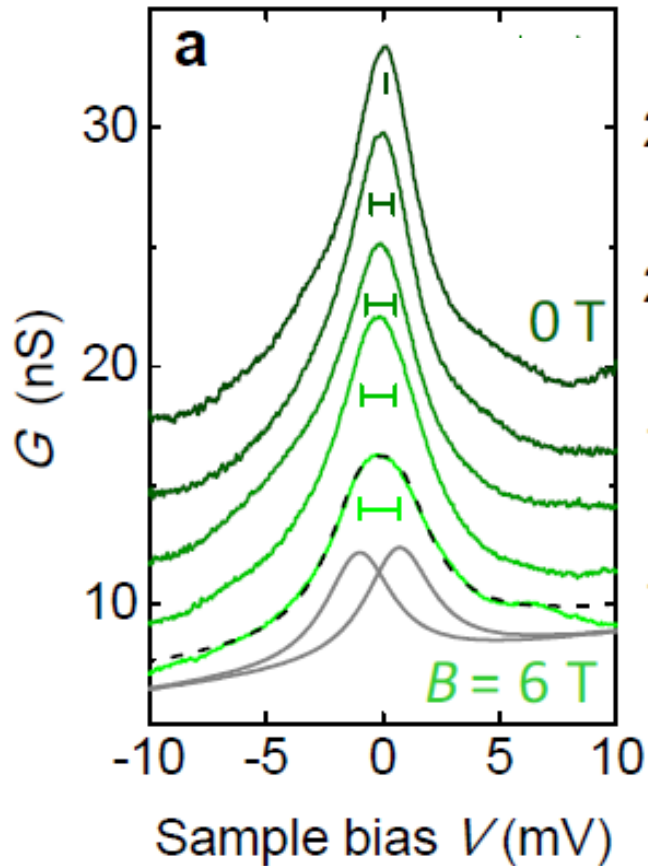


**There is no experimental control
over the position of these cobalt
atoms.**

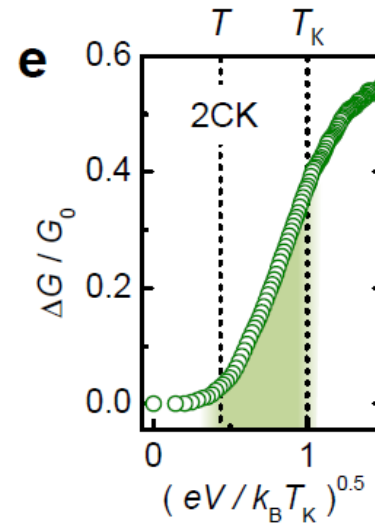
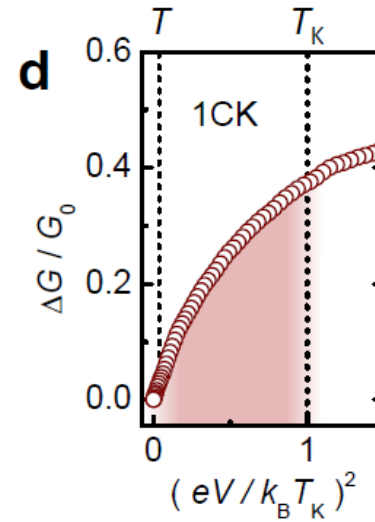
**The position of these atoms can be
accurately determined by STM
topography**

L. Mattos, *et al*, (unpublished)

Two channel Kondo physics: Impurity at hexagon center

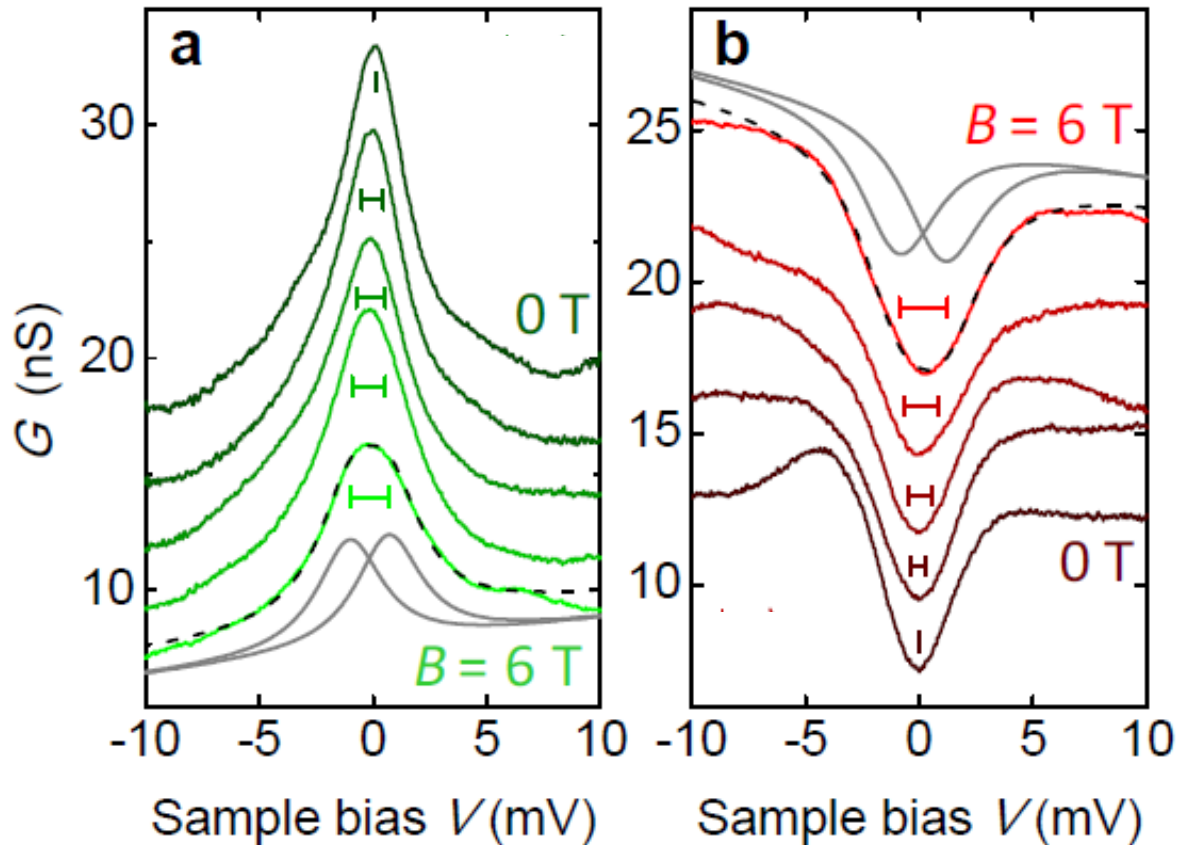


Observation of Kondo peak
in doped graphene sample
With $T_K = 16$ K



Proof of two-channel character of
the Kondo state: non-Fermi liquid
ground state in graphene.

Bimodal Spectra for the Conductance G

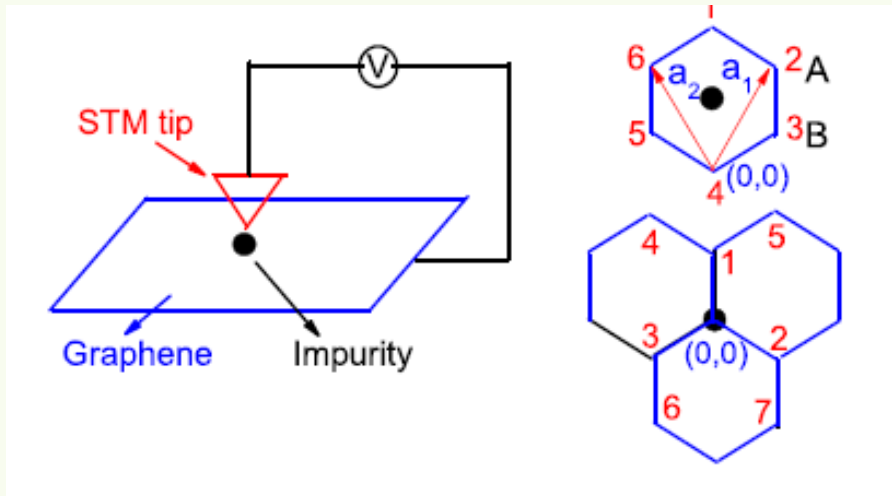


Impurity at the center: peaked structure of G and 2CK effect

Impurity on site: dip structure of G and 1CK effect

No analog in conventional Kondo systems: property of Dirac electrons

Theory of STM spectra in graphene



Model Hamiltonians for Graphene, Impurity and STM tip

$$\begin{aligned}
 H_G &= \int_{\vec{k}} \psi_s^{\beta\dagger}(\vec{k}) [\hbar v_F (\tau_z \sigma_x k_x + \sigma_y k_y) - E_F I] \psi_s^\beta(\vec{k}) \\
 H_d &= \sum_{s=\uparrow, \downarrow} \epsilon_d d_s^\dagger d_s + U n_\uparrow n_\downarrow \\
 H_t &= \sum_{\nu} \left[\sum_{\sigma=\uparrow, \downarrow} \epsilon_{t\nu} t_{\nu s}^\dagger t_{\nu s} + (\Delta_0 t_{\nu\uparrow}^\dagger t_{-\nu\downarrow}^\dagger + \text{h.c.}) \right] \quad (2)
 \end{aligned}$$

Tunneling current

Interaction between the tip, impurity and graphene:
Anderson model

$$H_{Gd} = \sum_{\alpha=A,B} \int_{\vec{k}} \left(V_{\alpha}^0(\vec{k}) c_{\alpha,s}^{\beta}(\vec{k}) d_s^{\dagger} + \text{h.c.} \right)$$

$$H_{dt} = \sum_{s=\uparrow,\downarrow;\nu} \left(W_{\nu}^0 t_{\nu s} d_s^{\dagger} + \text{h.c.} \right)$$

$$H_{Gt} = \sum_{\alpha=A,B;\nu} \int_{\vec{k}} \left(U_{\alpha;\nu}^0(\vec{k}) c_{\alpha,s}^{\beta}(\vec{k}) t_{\nu s}^{\dagger} + \text{h.c.} \right)$$

Tunneling current is derived from the rate of change of number of tip electrons

$$\mathcal{I}(t) = e \langle dN_t/dt \rangle = ie \langle [H, N_t] \rangle / \hbar$$

Obtain an expression for the current using Keldysh perturbation theory

$$G_{s,\alpha;\nu}^{\beta(1)<}(t; \vec{k}) = -i \langle t_{\nu}^{\dagger}(t) c_{s\alpha}^{\beta}(0; \vec{k}) \rangle$$

$$G_{\nu;s,\alpha}^{\beta(1)<}(t; \vec{k}) = -i \langle c_{s\alpha}^{\beta\dagger}(t; \vec{k}) t_{\nu}(0) \rangle$$

$$\mathcal{G}_{\mu\nu}^{(2)<}(t) = -i \langle t_{\nu}^{\dagger}(t) d_{\mu}(0) \rangle$$

$$\mathcal{G}_{\nu\mu}^{(2)<}(t) = -i \langle d_{\mu}^{\dagger}(t) t_{\nu}(0) \rangle$$

$$I(t) = \frac{e}{\hbar} \left[\sum_{\mu\nu} \left(W_{\mu\nu}^* \mathcal{G}_{\mu\nu}^{(2)<}(t) - W_{\mu\nu} \mathcal{G}_{\nu\mu}^{(2)<}(t) \right) + \int_{\vec{k}} \sum_{s\alpha\beta\nu} \left(U_{\alpha,s;\nu}^*(\vec{k}) G_{s,\alpha;\nu}^{\beta(1)<}(t; \vec{k}) - U_{\alpha,s;\nu}(\vec{k}) G_{\nu;s,\alpha}^{\beta(1)<}(t; \vec{k}) \right) \right]$$

**Turn the crank and obtain
a formula for the current**

Wingreen and Meir(1994)

$$\mathcal{I} = \mathcal{I}_0 \int_{-\infty}^{\infty} d\omega [f(\omega - eV) - f(\omega)] \rho_t(\omega - eV) \left[\rho_G(\omega) \times |U^0|^2 + \frac{|B(\omega)|^2}{\text{Im}\Sigma_d(\omega)} \frac{|q(\omega)|^2 - 1 + 2\text{Re}[q(\omega)]\chi(\omega)}{(1 + \chi^2(\omega))(1 + \xi^2)} \right]$$

**Contribution from
undoped graphene**

Impurity contribution

$$q(\epsilon) = [W^0/U^0 + V^0 I_1(\epsilon)]/[V^0 I_2(\epsilon)],$$
$$I_1(\epsilon) = -4(1 + \xi^2)(\epsilon + E_F) \ln |1 - \Lambda^2/(\epsilon + E_F)^2| / \Lambda^2$$
$$I_2(\epsilon) = 4(1 + \xi^2)\pi|\epsilon + E_F|\theta(\Lambda - \epsilon - E_F)/\Lambda^2.$$
$$B(\epsilon) = V^0 U^0 I_2(\epsilon)$$

**Shape of the spectra
depends crucially on
the Fano factor q
and hence on W^0/U^0**

U^0 coupling of graphene to tip

W^0 coupling of impurity to tip

V^0 coupling of graphene to impurity

**What determines the
coupling of Dirac
electrons to the STM
tip?**

What determines U^0

Bardeen Tunneling formula

$$U^0 \sim \int d^2r \left(\phi_V^\dagger(z) \partial_z \Psi_G(\vec{r}, z) - \Psi_G^\dagger(\vec{r}, z) \partial_z \phi_V(z) \right) \\ \sim \Psi_G(\vec{r}_0, z_0)$$

Tight-binding
wave-function
for graphene
electrons

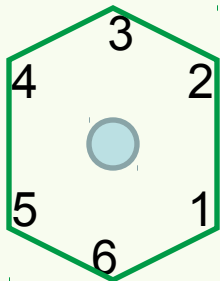


$$\Psi_G(\vec{r}, z) = \frac{1}{\sqrt{N}} \sum_{R_i^A} e^{i[\{\vec{K}(\vec{K}') + \delta\vec{k}\} \cdot \vec{R}_i^A]} \left[\varphi(\vec{r} - \vec{R}_i^A) \right. \\ \left. + e^{+(-)i\theta_k} \varphi(\vec{r} - \vec{R}_i^B) \right] f(z). \quad (1)$$

Plane-wave part

Localized p_z orbital part

Impurity on hexagon center



$$\sum_{R=1,3,5} \Psi_{A,s}^\beta(\vec{R}, z) = \sum_{R=2,4,6} \Psi_{B,s}^\beta(\vec{R}, z) = 0.$$

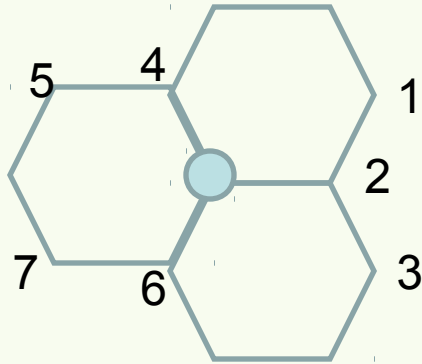
U^0 becomes small leading to large q .

$$q(\epsilon) = [W^0/U^0 + V^0 I_1(\epsilon)]/[V^0 I_2(\epsilon)],$$

**Peaked spectra for all
values of E_F independent
of the applied voltage**

Conductance spectra shows a peak for center impurities

Impurity on Graphene site



**Asymmetric position:
No cancelation and U^0
remains large**

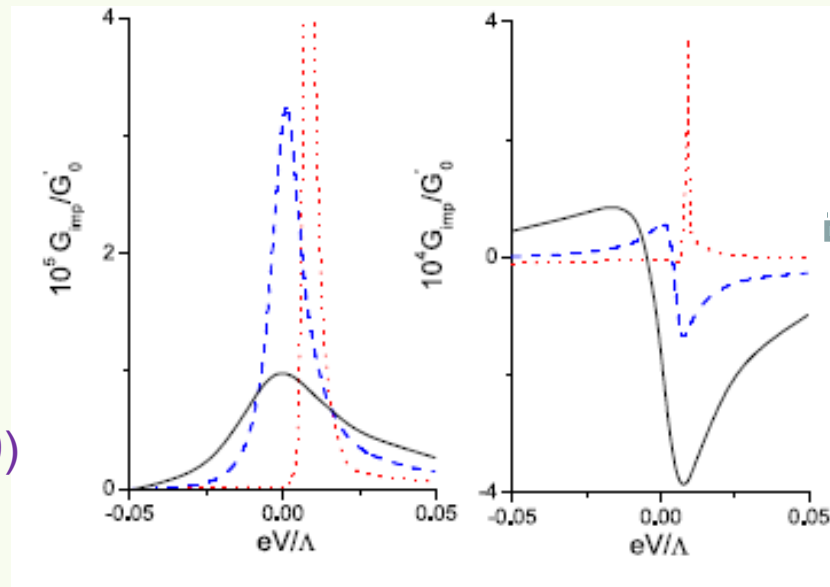
$$q(\epsilon) = [W^0/U^0 + V^0 I_1(\epsilon)]/[V^0 I_2(\epsilon)], \simeq I_1/I_2 \simeq -\ln|1 - \Lambda^2/(eV + E_F)^2|/\pi.$$

G should exhibit a change from peak to a dip through an anti-resonance with change of E_F

**Impurity on
hexagon center**



Refs: Saha *et al* (2009)
Wehling *et al* (2009)
Uchoa *et al* (2009)



**Impurity on
Graphene site**



**Should be observed
on surfaces of
topological insulators**

Conclusion

1. *The field of graphene has shown unprecedented progress over the last few years. First example of so called “Dirac materials”.*
2. *Several interesting physics phenomenon:*
 - a) *Dirac physics on a tabletop.*
 - b) *Unconventional Kondo physics*
 - c) *STM spectroscopy with Dirac fermions.*
3. *Potential applications in engineering:*
 - a) *Detection of gas molecules with great precision*
 - b) *Possibility of nanoscale room temperature transistors.*
4. *Future:*
 - a) *Controlled sample preparation and better lithography.*
 - b) *More strongly correlated phenomenon such as FQHE.*
 - c) *Graphene based electronics: future direction of nanotechnology?*